Multispectral imaging system on tethered balloons for optical remote sensing education and outreach

Joseph A. Shaw*[a], Paul W. Nugent[a], Nathan Kaufman[a], Nathan J. Pust[a], Devin Mikes [a], Cassie Knierim [b], Nathan Faulconer [a], Randal Larimer [a,c], Angela DesJardins[c], Berk Knighton[c,d]
[a]Electrical & Computer Eng. Dept., Montana State University, Bozeman, Montana, USA 59717;
[b]Physics Department, Montana State University, Bozeman, Montana, USA 59717;
[c]Montana Space Grant Consortium, Montana State University, Bozeman, Montana, USA 59717
[d]Chemistry and Biochemistry Dept., Montana State University, Bozeman, Montana, USA 59717

ABSTRACT

A set of low-cost, compact multispectral imaging systems have been developed for deployment on tethered balloons for education and outreach based on basic principles of optical remote sensing. The imagers use tiny CMOS cameras with low-cost optical filters to obtain images in red and near-infrared bands, and a more recent version include a blue band. The red and near-infrared bands are used primarily for identifying and monitoring vegetation through the Normalized Difference Vegetation Index (NDVI), while the blue band is used for studying water turbidity, identifying water and ice, and so forth. The imagers are designed to be carried by tethered balloons at altitudes up to approximately 50 m. Engineering and physics students at Montana State University-Bozeman gained hands-on experience during the early stages of designing and building the imagers, and a wide variety of university and college students are using the imagers for a broad range of applications to learn about multispectral imaging, remote sensing, and applications typically involving some aspect of environmental science.

Keywords: Multispectral imaging, remote sensing, optical system design, optics education, optics outreach

1. INTRODUCTION

Spectral imaging provides a wide array of opportunities for students to gain experience with and learn about light, the interaction of light with natural objects, and the use of digital imaging systems in remote sensing for studying the natural environment. We adopted this as a theme for a NASA minority-serving-institution partnership project involving Montana State University (MSU) in Bozeman, Montana, and seven Native American Tribal Colleges in Montana (Blackfeet Community College, Salish Kootenai College, Fort Belknap College, Stone Child College, Fort Peck Community College, Little Big Horn College, and Chief Dull Knife College). The goals of the project were for a team of undergraduate students at MSU-Bozeman to design and build eight copies of a two-channel spectral imager and deliver them with complete documentation to the Tribal Colleges, where students would use the imagers in environmental science projects with financial support from NASA through the Montana Space Grant Consortium.

The imaging systems developed in this project were to be built with a parts cost no greater than $1,000 US, and provide simultaneous images in the red and near-infrared portions of the spectrum from a tethered balloon that rises to an altitude of approximately 50 m (above which FAA clearance is required). The requirement for simultaneous images is driven by the instability of the balloon platform, which would make it very difficult to align images in different spectral bands if they were acquired with any significant time delay. It was desired for the operators on the ground to have the ability to view images in real time and to trigger image acquisition when the desired scene was in the imager's field of view. The balloon payload was limited to 2.3 kg, and it was desired to operate each imager for one hour or longer without charging batteries. Finally, a ground-based calibration target was required for each imager, thereby enabling real-time calibration of the images to determine the reflectance at each pixel.

* jshaw@ece.montana.edu; phone 1 406 994-7261; fax 1 406 994-5958; www.coe.montana.edu/ee/jshaw

Optics Education and Outreach II, edited by G. Groot Gregory, Proc. of SPIE Vol. 8481
84810T · © 2012 SPIE · CCC code: 0277-786/12/$18 · doi: 10.1117/12.932236

2. IMAGING SYSTEM DESIGN

The low-cost, balloon-based imaging systems designed in this project were inspired by our use of multispectral imaging of vegetation for detecting CO_2 gas leaks through the resulting reflectance changes.[1-3] Hyperspectral imaging also has been employed for similar purposes.[4-6] This research was conducted at an agricultural field west of the MSU-Bozeman campus, with support through the Zero Emissions Research and Technology (ZERT) center at Montana State University.[7] In our multispectral imaging experiments at the ZERT site, we acquire red and near-infrared (NIR) reflectance images of the vegetation, and then identify the locations of leaking gas through statistical analysis of the reflectances and the Normalized Difference Vegetation Index (NDVI), calculated as follows:

$$NDVI = \frac{\rho_{nir} - \rho_{red}}{\rho_{nir} + \rho_{red}}, \quad [1]$$

where ρ represents the reflectance for red and near-infrared (nir) bands, corresponding to approximately 630-680 nm and 770-820 nm, respectively.[2] Because of chlorophyll absorption, healthy vegetation absorbs in the red and reflects strongly in the NIR, beyond the so-called "red edge" at 700 nm.[8] Reflectance spectra for healthy and stressed vegetation are illustrated in Figure 1, showing that for stressed vegetation the red reflectance rises while the NIR reflectance falls. Therefore, a high NDVI value indicates healthy vegetation, and because of a much flatter red-NIR transition, smaller or even negative NDVI values can indicate the presence of a material ranging from stressed vegetation to urban materials.

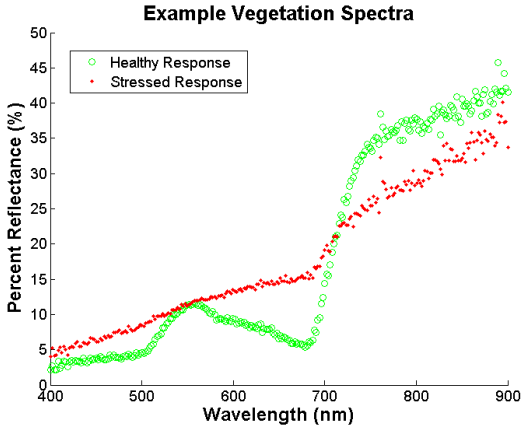

Figure 1. Visible and near-infrared reflectance spectra for healthy vegetation (green circles) and stressed vegetation (red dots).

The balloon-borne imagers were designed to allow students to explore the use of the NDVI and related reflectance-based remote sensing in the red and near-infrared spectral region. The response of the imagers can be moved to other spectral bands by replacing the optical filters that are situated directly in front of the ultra-low-cost CMOS cameras.

Figure 2 is a photograph of one of the imaging systems that was built at MSU-Bozeman for use at a Tribal College. The two circular objects near the left of this picture are optical filters that define the two spectral bands. These filters are optically sealed to the front of the lenses of two tiny CMOS cameras. Just to the right of the cameras and filters is a nickel-metal-hydride (NiMH) 12-v battery, and to the right of that are the electronics boards. The two boards at the top right of the picture are used to record images from each camera onto two SD cards, and the bottom-right board contains a consumer-grade webcam removed from its housing. This webcam provides a live view that is transmitted to the ground via a 2.4-GHz wi-fi link that uses the black antenna in this picture. The white antenna on the front side is for a wi-fi link that allows the ground-based operator to trigger image acquisition through a dual-channel 2.4 GHz ZigBee relay.

In a second phase of the project, we designed and built an enhanced version of the balloon-borne multi-spectral imager with a blue-green channel along with the original red and NIR ones (Figure 3). This second-generation system also had a significantly improved live balloon-to-ground video link and an even lower weight (1.0 kg, compared to 1.45 kg for the 2-channel imager) and longer battery life (~3 hr, up from ~2). The new system uses a 5.8-GHz video transmitter to send the live video from one of the three CMOS cameras. A

three-way switch on the imager module is used while the imager is on the ground to select which camera's output is viewed on the live video feed. An operator then uses a laptop computer with a wi-fi transmitter and custom software to trigger an image acquisition when the camera's field of view contains the desired object.

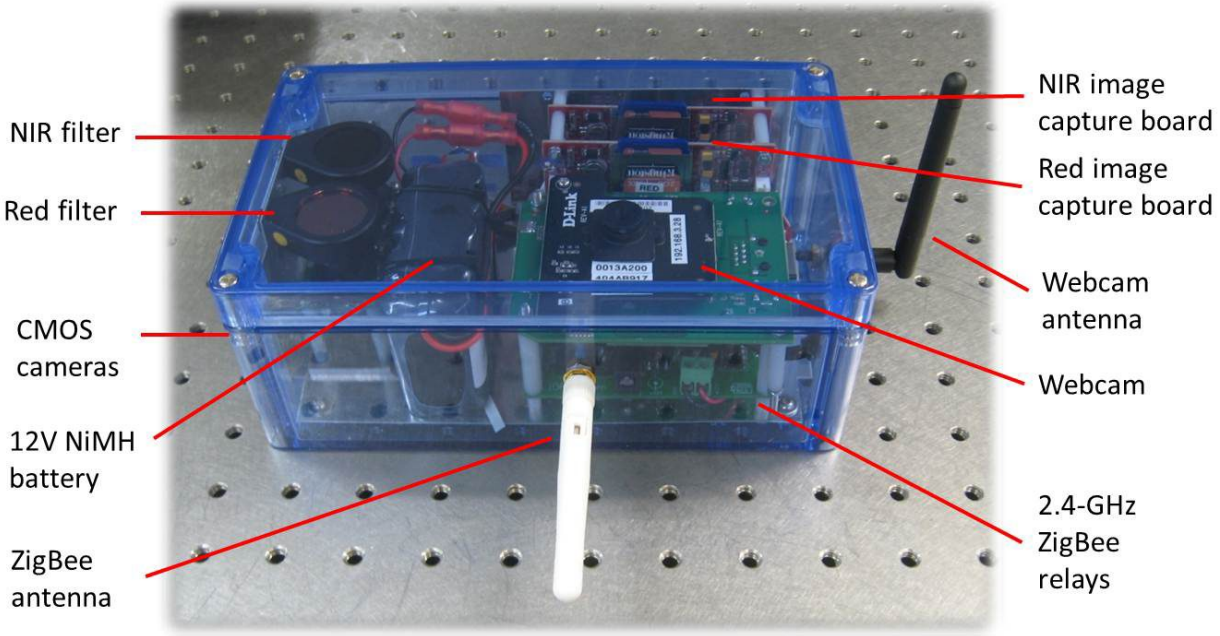

Figure 2. Photograph of original two-channel, balloon-borne, multispectral imager with primary subsystems labeled.

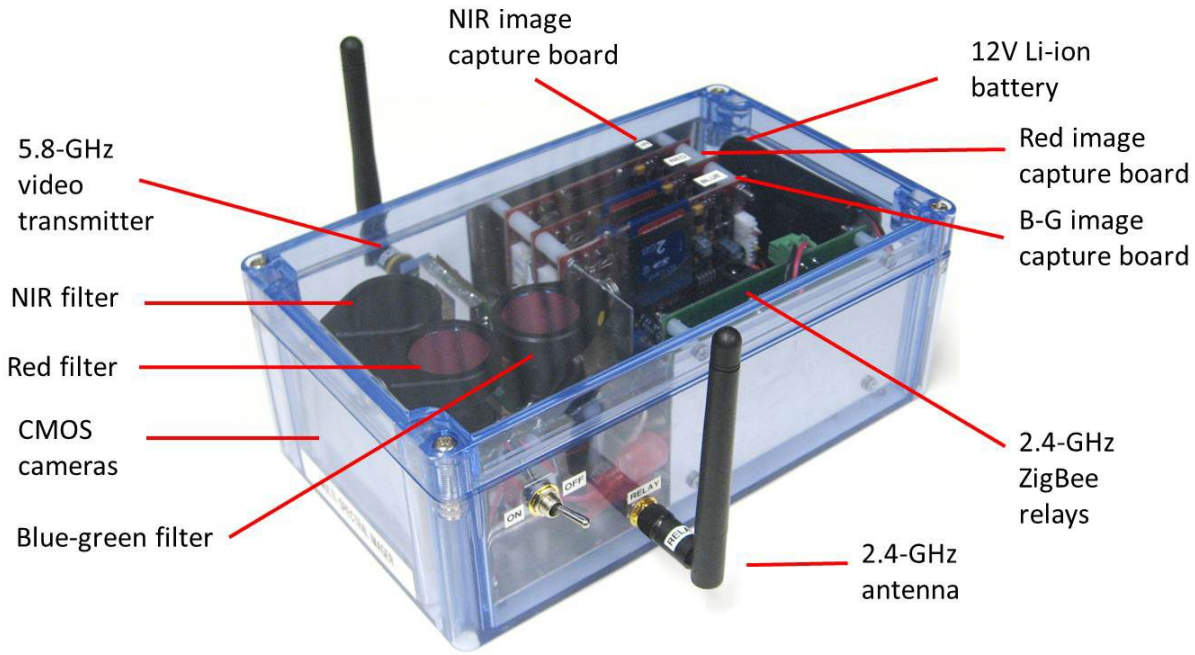

Figure 3. Photograph of second-generation, three-channel imager with primary subsystems labeled. This version has three spectral channels: blue-green, red, and NIR.

Because the tethered balloon is flown at a relatively low altitude (~50 m), we chose cameras and lenses with a wide-angle field of view. The chosen camera was from Electronics123 (model M3186A, cost = $27.50 US) with a full-angle field of view approximately equal to 65°×50° with 510×492 pixels. Therefore, with the

balloon at 50 m altitude, the imager could see an area on the ground with approximate dimensions of 64×46 m, with approximately 12-cm pixel resolution at the ground.

Although the wide-angle field of view is convenient for imaging relatively large areas, such large incident angles cause the spectral response of interference filters to shift toward shorter wavelengths with a distorted filter response curve. Therefore, interference filters must be avoided whenever possible. This also is in accordance with the need to minimize cost, as interference filters can be fairly costly. Our solution was to use gel filters wherever possible. Gelatin filters can be purchased at low cost at photographic supply stores, and have quite wide spectral response with effectively zero angle dependence. We used a commonly available visible-block, NIR-pass, filter to define the short-wave cutoff of the NIR channel, as shown in Figure 4a. The long-wave cutoff for this filter (not shown in the figure) is established at approximately 1000 nm by the CMOS camera response, which typically decays rapidly beyond about 900 nm for silicon detectors.[9] The red channel was more problematic, as the standard red gel filter transmits both red and NIR. Therefore, we stacked the red gel filter with two NIR-blocking interference filters that pass wavelengths shorter than 700 nm. The product of these transmission curves produces a red band-pass filter with half-power transmission wavelengths of approximately 620 nm and 670 nm, as shown with the center blue line in Figure 4b (this was still lower cost than purchasing an equivalent red band-pass interference filter).

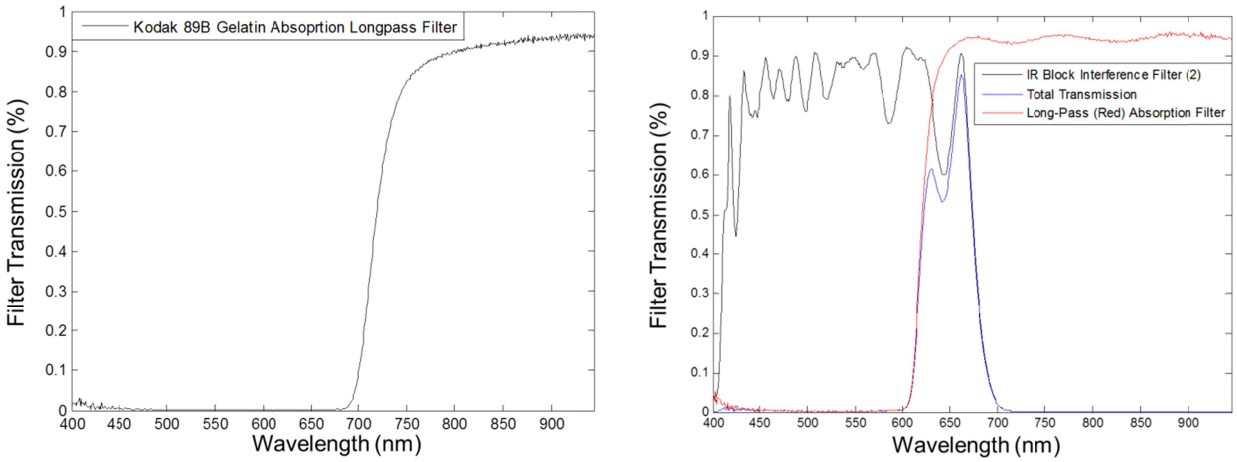

Figure 4. Spectral transmission functions for the (a) NIR filter and (b) red filter, comprising an IR-block filter (left curve shown in black) stacked with an IR-pass filter (right curve shown in red). The center curve shown in blue is the net on-axis red transmittance.

Because we had to use an interference filter to remove the NIR portion of the red gel filter transmittance, pixels at the edge of the field of view experienced a red-channel transmittance that was generally lower in amplitude and shifted to slightly shorter wavelengths. We accounted for this by measuring the net filter transmittance spectrum using a spectrometer, while the filter was rotated to different angles in front of a uniformly illuminated integrating sphere. The measured angle-dependent response was compensated for using custom image-processing software written by the undergraduate student team.

Figure 5 illustrates an important lesson for students to learn in this type of project. Quite often, a band-pass filter that appears as a certain color to a human observer includes “out-of-band” transmittance at a totally different, often invisible, spectral region. This was the case with the blue-green gel filter, whose transmittance curve is shown in Figure 5. It has a nicely defined blue-green band with approximate half-power wavelengths of 440 nm and 540 nm, but it has an even higher transmittance at NIR wavelengths beyond 700 nm. Therefore, we combined the blue-green gel filter with two more of the NIR-blocking filters used in the red channel, resulting in a blue-green channel with zero NIR response, as shown in Figure 5.

The low-cost CMOS cameras use automatic gain control to continually adjust for the varying brightness levels observed in the scene. Because there is no way to turn off or to control this feature on these cameras,

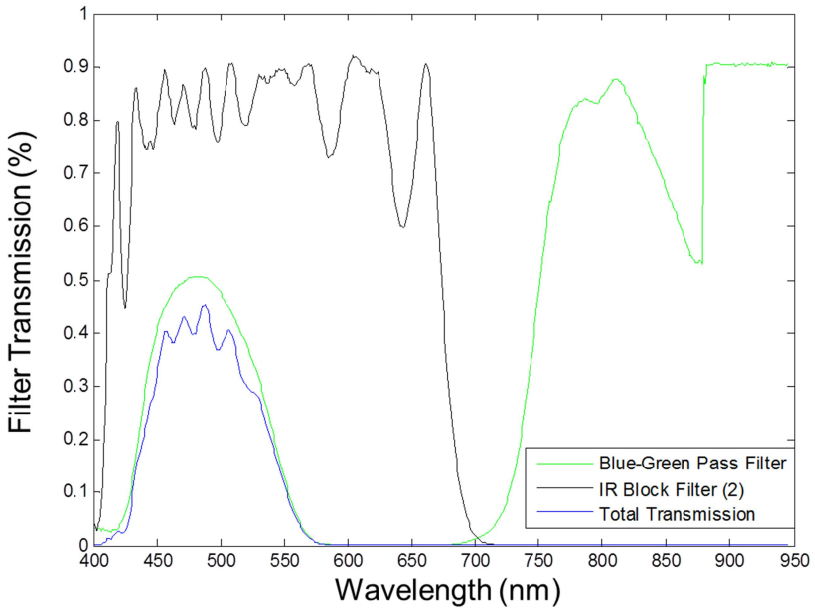

Figure 5. Spectral transmission function for the blue-green channel in the second-generation imager system. Similar to the red channel, this filter is comprised of stacked IR-block and green-pass filters. The net blue-green response is the lower-left curve.

it was necessary to use a ground-based calibration target to turn the recorded image digital numbers into reflectance values. An early example, shown in Figure 6, was constructed by painting the two halves of a plywood sheet black and white. Later calibration targets were made by painting canvas tarps, which allow much easier transport to a measurement site. The reflectance spectrum was measured for the black portion and the white portion, using a hand-held spectrometer and a Spectralon 99%-reflective calibration reference target. The image-processing software incorporates these measured spectra and uses them, along with the measured filter response curves, to calculate the reflectance for each pixel of each image. However, because of the large amount of angular response falloff inherent in these low-cost cameras, this approach also required that we use a uniform integrating-sphere source to create a map of camera response vs pixel number. This map also is incorporated in the image-processing software to relate the other image pixels to the pixels containing the black and white calibration reference regions.

Figure 6. Photograph of a plywood black-and-white reflectance calibration panel, which is laid on the ground within the imager's field of view to provide a reflectance calibration. Later versions were painted on canvas tarps.

Table 1 lists the primary components used in the second-generation multispectral imaging system, which provided 3 channels instead of 2, in a package that was much lighter than the original system with longer battery life. The table also includes nominal specifications and cost for each component. All components are in the imaging system except the ZigBee coordinator and 5.8-GHz receiver, which are used on the ground with the laptop computer to provide communication with the balloon-borne imager. The table does not include items such as the case, switches, wires, connectors, and so forth. With everything included, the total parts cost for the second-generation, three-channel multispectral imaging system was $1,100US. The two-channel systems used parts that cost less than $900.

Table 1. Parts list for the second-generation multispectral imaging system with nominal specifications and cost

Component	Specifications	2010 cost	Quantity
M3186A CMOS camera (Electronics123)	200 mW max, 3.7-mm f/2 lens, ~65°×50° FOV, 1/60 – 1/15,000 s integration time, 510×492 pixels	$27	3
DVR8106 recording module (Electronics123)	1.8 mW max, 2 GB SD card, 320×240 video, 640×480 still image capture	$60	3
SD card	2 GB	$6	3
ZR25_ZBMESH ZigBee relay (National Control Devices)	single-pole double-throw	$93	1
ZBU_COORD ZigBee coordinator (National Control Devices)	5V USB input	$138	1
NTX100 5.8-GHz video transmitter (Ifrontech)	6-15 VDC, ~92 mA	$100	1
NRX Nano 5.8-GHz receiver	6-15 VDC, <200 mA	$145	1
Li-ion battery for remote module	10.8 VDC, 2400 mAh	$79	1
NiMH battery for video receiver	12 VDC, 2600 mAh	$30	1
Rosco 38000 IR/UV block filter	1” diameter	$6	4
Kodak #29 dark red wratten gel filter	100 mm square sheet → 16 filters	$54	1
Kodak #89B NIR pass gel filter	100 mm square sheet → 16 filters	$108	1
Kodak #44A blue-green gel filter	75 mm square sheet → 16 filters	$95	1

3. EXAMPLE DATA

Nine multispectral imager systems were built and are being used by a wide variety of students for a broad range of applications, but here we show example images obtained during an outreach event with Native American middle-school students at MSU-Bozeman. The imager was attached to a helium-filled balloon and tethered at an altitude near 50 m on the south side of the MSU campus in a region containing a mixture of grass, cement sidewalks, and asphalt streets, as shown in the photograph of Figure 7. In this photograph, the balloon is near the top, slightly to the right of center, the black-and-white reflectance calibration panel is near the bottom of the picture, just right of center, and the students using a laptop computer with wireless link to control the camera are near the lower left.

Figure 7. Photograph of tethered balloon carrying multispectral imager during test flight at Montana State University. The tethered balloon is located just right of the upper center, while the calibration panel is at the bottom center, next to a parked car.

Figure 8 shows red and NIR images acquired simultaneously by the balloon-borne imager during this test flight. These images show several features that can be related immediately to the reflectance spectra of the various regions on the ground. For example, the grass along the lower and upper edges is dark in the red image and very bright in the NIR image, as expected from the reflectance spectra shown in Figure 1. Also, the asphalt street at the center of the image is notably brighter in the red than in the NIR. A similar behavior is observed for the cement sidewalk above and below the asphalt street (with strips of grass on either side). The circular dark region near the upper-right corner of the images is the shadow of the balloon.

The images were retrieved by lowering the balloon, extracting the SD cards, and reading them with the control computer. Once the images were stored on the computer, the image-processing software was used to perform a reflectance calibration. The same image-processing software was also used to align the red-NIR image pairs and to select the pixels containing the black and white calibration panel regions. With all of these steps completed, the software was used to calculate the NDVI at each pixel. The resulting NDVI image for this example is shown in Figure 9, with a color bar that ranges from dark blue denoting NDVI = -1 to dark red denoting NDVI = +1. This image shows an NDVI pattern that can be explained by the relative dark and bright regions of the images shown in Figure 8. For example, the grass regions have large, positive NDVI, while the asphalt and concrete regions have large, negative NDVI (indicating that these materials are more highly reflective in the red than in the NIR). Because both the black and white regions of the reflectance calibration panel have a relatively flat reflectance spectrum, the NDVI is near zero for both of these regions. The dark strip along the bottom of the NDVI image is where pixels have been ignored after shifting one image with respect to the other to achieve very accurate pixel alignment. Imprecise alignment will result in an edge-detection image because of the subtraction in the NDVI calculation.

Figure 8. Images acquired from the balloon-borne multispectral imager: (a) red and (b) NIR.

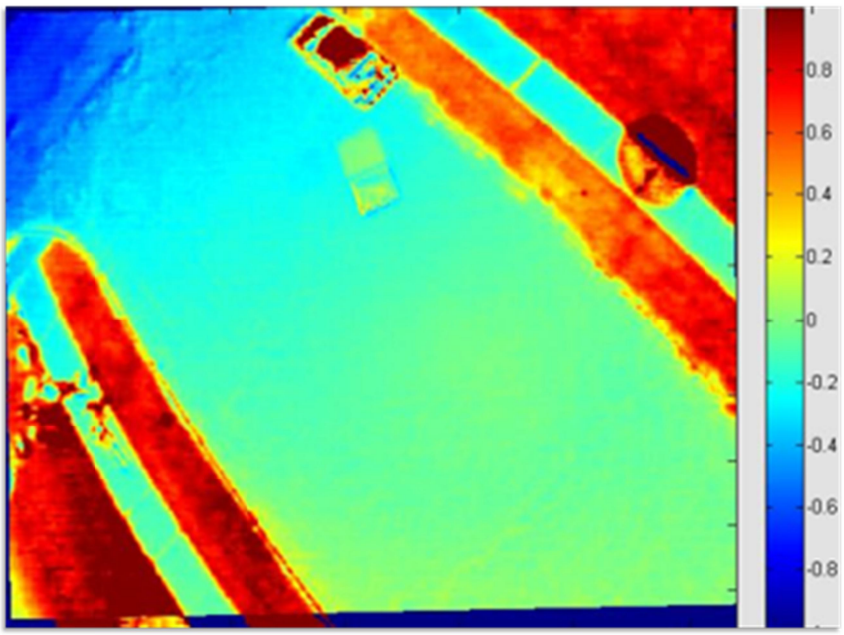

Figure 9. Normalized Difference Vegetation Index (NDVI) image produced from the red and NIR images in Figure 8.

4. CONCLUSION

A low-cost, multispectral imaging system was designed and nine copies built by undergraduate students majoring in electrical engineering, computer engineering, and physics at Montana State University. These imagers, especially the second-generation, three-channel system, provide a useful and effective mechanism to teach principles of optical engineering, imaging, and remote sensing. The imagers operate on a tethered balloon at altitudes up to approximately 50 m. Initial data demonstrate the capability of these low-cost imagers for scene classification using the Normalized Difference Vegetation Index to identify vegetation and non-vegetation regions. Future research will explore their use in quantitatively demanding studies that use the NDVI as a measure of plant health.

REFERENCES

[1] Rouse, J. H., Shaw, J. A., Lawrence, R. L., Lewicki, J. L., Dobeck, L. M., Repasky, K. S., and Spangler, L. H., "Multi-spectral Imaging of Vegetation for Detecting CO_2 Leaking From Underground," Env. Earth Sci., 60(2), 313-323 (2010).

[2] Hogan, J. A., Shaw, J. A., Lawrence, R. L., and Larimer, R. M., "Low-cost multispectral vegetation imaging system for detecting leaking CO_2 gas," Appl. Opt., 51(4), 59-66 (2012).

[3] Hogan, J. A., Shaw, J. A., Lawrence, R. L., Lewicki, J. L., Dobeck, L. M., and Spangler, L. H., "Detection of leaking CO_2 gas with vegetation reflectance measured by a low-cost multispectral imager," IEEE J. Selected Topics Appl. Earth Obs. Remote Sensing, 5(3), 699-706 (2012).

[4] Keith, C. J., Repasky, K. S., Lawrence, R. L., Jay, S. C., and Carlsten, J. L., "Monitoring effects of a controlled subsurface carbon dioxide release on vegetation using a hyperspectral imager," *Int. J. Greenhouse Gas Control,* 3, 626–632 (2009).

[5] Male, E. J., Pickles, W. L., Silver, E. A., Hoffmann, G. D., Lewicki, J. L., Apple, M., Repasky, K. S., and Burton, E. A., "Using hyperspectral plant signatures for CO_2 leak detection during the 2008 ZERT CO_2 sequestration field experiment in Bozeman, Montana," Env. Earth Sci., 60(2), 251-261 (2010).

[6] Bellante, G. J., "Hyperspectral remote sensing as a monitoring tool for geological carbon sequestration," M.S. thesis Montana State University, Bozeman, 2011, http://etd.lib.montana.edu/etd/view/item.php?id=1440.

[7] Spangler, L. H., Dobeck, L. M., Repasky, K. S., Nehrir, A. R., Humphries, S. D., Barr, J. L., Keith, C. J., Shaw, J. A., Rouse, J. H., Cunningham, A, B., Benson, S. M., Oldenburg, C. M., Lewicki, J. L., Wells, A. W., Diehl, J. R. , Strazisar, B. R., Fessenden, J. E., Rahn, T. A., Amonette, J. E., Barr, J. L., Pickles, W. L., Jacobson, J. D., Silver, E. A., Male, E. J., Rauch, H. W., Gullickson, K. S., Trautz, R., Kharaka, Y., Birkholzer, J., Wielopolski, L., "A shallow subsurface controlled release facility in Bozeman, Montana, USA, for testing near surface CO_2 detection techniques and transport models," Env. Earth Sciences, 60(2), 227-239 (2010).

[8] Jensen, J. R., [Remote Sensing of the Environment: an earth resource perspective], Prentice-Hall Publishers, Upper Saddle River, NJ, ch. 10 (2000).

[9] Dereniak, E. L. and G. D. Boreman, [Infrared detectors and systems], John Wiley & Sons Publishers, New York, NY (1996).